Peer Review File

Manuscript Title: Molecular Architecture of Coronavirus Double Membrane Vesicle Pore Complex

Reviewer Comments & Author Rebuttals

Reviewer Reports on the Initial Version:

Referees' comments:

Referee #1 (Remarks to the Author):

Huang et al. present the cryo-electron tomography (cryo-ET)-based structure of the protein pore that was previously found to form in double-membrane vesicles (DMVs) of the SARS-CoV-2. The authors reconstituted DMVs and pores in cells transfected with a fusion of Nsp3 and Nsp4 proteins, which build up the pore, purified the DMVs, collected a large amount of cryo-ET data, and obtained cryo-ET maps at local resolutions ranging from 3.7Å to 7.1Å. Then, they built a structural model based on the maps. They used the models to explain how the pore is built up, how the pore for RNA translocation might be formed, and what might be critical domains and residues for pore stability. Based on the model, they also predicted residues important for RNA translocation and confirmed that using recombinant viruses.

Overall, this is an impressive work in the methodology and results, and has the potential to be a seminal paper in the SARS-CoV-2 and cryo-ET fields. The pore has been identified before, but the previous cryo-ET maps were of very low resolution, and at most, partial and approximate structural models could be proposed (Wolff, 2020; Zimmermann, 2023). The manuscript reads very well, and the figures are clear. The structure is compared to the prior data and pores of other viruses. The structure is fascinating in how the rings of the pore are assembled, how they interact with the membrane, and how the symmetry changes along the axis of the pore. While the comparison to the nuclear pore complex may seem tangential, it offers an interesting perspective for understanding the functional dynamics of double-membrane-spanning pores.

Major comment:
In its current form, the manuscript does not allow for assessing the quality of the structural model, even though a very well-prepared set of cryo-ET maps, local resolution maps, and structures have been provided in the additional data for review. I am aware that many publications do not include such an assessment, but in the opinion of this reviewer, this is necessary.
The following information needs to be provided:
- Local quality of fits to the cryo-ET maps. Several tools are available for that, such as Q-scores (https://www.nature.com/articles/s41592-020-0731-1), SMOC (https://www.ncbi.nlm.nih.gov/pmc/articles/PMC4854230/), and DAQ (https://github.com/kiharalab/DAQ). The high-resolution regions should be checked for sequence registers using tools like checkMySequence (https://pubmed.ncbi.nlm.nih.gov/35775980/) to have a more quantitative assessment than the visual Extended Data Fig. 6. The authors could use tools as above and provide figures with the scores mapped to the structural model.

- Assessment of overfitting. Several regions of the cryo-ET map have only medium resolution in which side chains are not visible. Placing and refining AlphaFold models in those regions with COOT/ISOLDE may lead to distortions of the starting models and overfitting to the map. To let the reader assess the overfitting, the final model needs to be compared to the starting partial models. This could be done by using figures with side-by-side comparisons, and, ideally, mapping LDTT scores (https://www.ncbi.nlm.nih.gov/pmc/articles/PMC3799472/) on the final model, or plotting per-residue LDDT and local resolution of the cryo-ET map side by side (in case of overfitting, low local resolution regions would coincide with low LDDT).
- Quality assessment of the starting AlphaFold models. AlphaFold models always come with predicted quality scores, both global and local. These need to be shown. Global pTM and ipTM (if any Nsp3-Nsp4 complexes were modeled) scores should be reported in a table. Models colored by the local pLDDT score should be used. PAE plots should be shown, regardless of whether Nsp3 and Nsp4 were modeled individually or together.
- More detailed explanation of the modeling procedure. Currently, it is not possible to understand which regions were modeled de novo, which based on the AlphaFold models. The membrane helices seemed to be done denovo, but were the initial helices taken from AlphaFold or traced manually in Coot? Also, were the Nsp3 and Nsp4 domains modeled with AlphaFold as monomers or as subcomplexes? Which regions were refined in Coot/ISOLDE, and which were kept rigid? Which of the multiple maps obtained were used for building the models?
- Explanation of: If the model was built by fitting individual domains of Nsp3 and Nsp4 manually, how the interfaces between the domains were refined, and how were the clashes removed? Note that shifting side chains or a backbone with ISOLDE at low resolution to remove clashes may lead to artificial distortions and, thus, incorrect models. Even if that was the case, and authors want to keep it at that precision, this needs to be reported and would also be clear to the reader when the above overfitting measures are provided.
Please note that Extended Data Table 1 is necessary to report but does not provide information for addressing the above points. It only reports on the geometrical quality of the structures, which does not exclude overfitting to maps or deviations from the starting structures.

Minor comments:
- Indicate the prongs in Figure 1 to clarify their identification for the reader.
- Page 2, lines 63-63: “Our structure reveals an unexpected stoichiometry” – it should be explained why the revealed stoichiometry was “unexpected”.
- The Nsp3-4 has been expressed as a tandem polypeptide. Could the authors elaborate in the manuscript why they think this does not change the structure of the pore?
- In Figure 3f, the coloring does not seem to correspond to the other panels; perhaps it could be made consistent for better orienteering.
- ISOLDE is not listed in the Reporting Summary
- It would be highly appreciated if the raw tilt series were deposited in the EMPIAR database.
- What the B-factor values in the provided PDB files correspond to?

Referee #2 (Remarks to the Author):

In infected cells, coronaviruses induce an elaborate network of modified host (double) membranes, of which double-membrane vesicles (DMVs) have been identified as the central hub for viral RNA synthesis. Specific membrane-spanning coronavirus replicase subunits (nsp3, nsp4 and nsp6) have been implicated in the formation and structure of DMVs, which – a couple of years ago - were found to contain membrane-spanning pores that are now thought to play a critical role by enabling the export of viral RNA produced inside the DMVs to the cytosol for translation and encapsidation into new virions.

This exciting study reports sub-nm structures of the pore complex spanning the DMVs that are induced following the expression of the coronavirus nonstructural proteins nsp3 and nsp4. Affinity purification of these DMVs, cryotomography and subtomogram averaging provided several density maps of the DMV-spanning complexes. Using pre-existing domain X-ray structures and AlphaFold, the authors construct structural models offering unprecedented insight into the core architecture of these pores and revealing them as made of 12 copies of each nsp3 and nsp4 organized in stacking hexameric rings. The structure suggests novel hypotheses on pore formation and function, and additional mutagenesis experiments included in this study align with these hypotheses. While the question of whether the pore complex reported here is identical to that formed in DMVs in infected cells remains open, this work represents a major step forward to understanding the structural basis of the DMV-spanning pore complexes.

While the significance of this study is undeniable, there are some issues that require attention, particularly regarding unresolved masses in the structures:

• The primary concern revolves around the absent masses in both nsp3 and nsp4 across all the structures. Even the complex the authors name “full pore complex” is solved as nsp3L:nsp3S:ns4L:nsp4S (6:6:6:6), with nsp3S lacking the entire N-terminal cytosolic domain, which represents approximately 50% of the total nsp3 mass (~100 kDa). Even larger parts of the proteins are missing in the smaller reported structures (“consensus pore” and “extended pore”). The lack of clarity surrounding this issue is compounded by the complete absence of an explanation for the underlying reasons. Potential explanations may include:

(1) Structural flexibility of these domains, which may result in missing masses in the averaged structures. However, these masses probably are discernable in the individual complexes within the tomograms. Therefore, the fact that individual small pores (“consensus pores”) are pointed out in the raw data in Fig. 1a seems to exclude this hypothesis. Yet, the figure is too small, and I propose that a series of individual pore galleries showcasing the three different types (full pore, extended pore, consensus pore) is presented to better assess this point. In a similar vein, the extended pore structure, omitted from Fig 1a, is it a somewhat artificial product of image processing or does it represent a genuine entity in the DMVs?

(2) The actual existence of shorter forms of nsp3. (The Western blots in Extended data figure 1 may suggest this option?). If so, is this biologically significant or merely a result of degradation during purification? How does it align with the previous knowledge about nsp3? Considering the nsp3-4

expression system used, could this be a product of splicing, which would not be relevant in the context of cytosolic replication during viral infection?

• Another critical (but small) mass not resolved or mentioned is the hydrophobic N-terminal domain of nsp4: residues 1-30, with residues 10-30 being a predicted TM domain, and a domain that is liberated by the nsp3/4 cleavage, which must occur on the cytosolic side of the membrane. It remains entirely unclear why this region has not be resolved, warranting attention in the article. Its omission in Fig.2a renders the figure confusing. Given that nsp3-4 are expressed as a single polypeptide, the N-terminal domain of nsp4 must (at least initially) be cytosolic, with the nsp3-4 junction accessible to the PLpro domain of nsp3 for cleavage.

• Notice that, without this pivotal N-terminal nsp4 segment that should cross the membrane, the luminal orientation of the nsp4 ecto domain would not be possible, and therefore it is critical for the proposed model of pore formation through cis-oligomerization of the nsp3 end nsp4 ectodomains (l. 208-215) and the membrane zippering through trans-interactions. I strongly encourage the authors to include a schematic illustration of this model as an Extended figure and in the context of DMV formation, as this would be extremely informative. If space restrictions apply, this figure could substitute Extended Data Figure 10, which, in my view, conveys little information.

• Note also that the existence of this additional nsp4 TM segment has implications for the nomenclature of the nsp4 TM helices resolved, which would be TM2-TM6 rather than TM1-TM5. It would seem important not to create nomenclature confusion in this (potentially) seminal publication, which will likely be a reference point for many future studies. Likewise, the reason to call TM4 of nsp3 a TM domain is not very clear, as the domain does not seem to be spanning the membrane (Fig. 2a). It should be considered to name it differently as many will assume that the number of TM domains (even or odd) automatically defines whether the N- and C- termini of nsp3 are on the same or opposite sides of the membrane.

• Another puzzling aspect of the structure is the considerable distance between the NAB and TM1 regions of nsp3L, situated essentially on opposite sides of the pore (see, for example, Fig. 2f), while only separated in the sequence by the βSM domain. It remains unclear how this unresolved domain could bridge this distance, as this is not addressed in the article.

Mutagenesis experiments:

• Negatively charged mutations introduced in the ectodomain of nsp3 seem to impede or reduce the interaction with nsp4, nicely supporting the author's model (Fig. 3i). However, and despite the absence of mutations in nsp4, the input gel shows poor expression and double bands for nsp4, a factor that could potentially affect the main claim.

• The second set of mutagenesis experiments summarized in Extended Data Fig. 9 align with the suggested notion that the charged residues inside the channel of the structure are critical for viral replication. Importantly, however, the rescue experiment with recombinant mutant viruses in panel b appears to lack a positive control (wt), which would be critical to exclude issues with the experimental setup.

• Given the potential influence of unrelated factors on the outcomes of both sets of mutagenesis experiments, it would be important to assess the structures formed (DMVs? paired membranes? pores?) in one or two selected mutants using the expression system. This step would significantly contribute to strengthen the conclusions.

Others:
• A point not directly addressed in the text is the possible disparities with the pore complexes formed in infection. The lack of e.g. RdRp and RNA synthesis, and the potential consequences should be pointed out to the reader. In this regard, l. 22 in the abstract referring to "SARS-CoV-2 pore complex" is misleading –maybe use nsp3-4 complex, as in the rest of the text.

• The claim in line 60 should be tempered, as it appears premature; at present, it stands as an exciting and plausible yet hypothetical model. Note that, as indicated in the previous point, there is not RNA in the nsp3-4 protein expression system.

• L. 249-250. For another betacoronavirus (MHV, mouse hepatitis virus), a nsp4 mutant with a ~100 amino acid C-terminal deletion has been reported to be viable (Sparks et al. 2007, PMID: 17855548), which may argue against this hypothesis.

• For the sake of clarity for non-expert readers, the pore complexes in the neck of the spherules that are induced by other viruses, such as nodaviruses or alphaviruses, and which appear in results and figures, should already be mentioned in the introduction.

• Please, indicate the transfection efficiency in the purification setup. Was GFP added as a tag to the nsp34 construct to assess this point? Right now, the reason behind its inclusion in the constructs is unclear.

• L. 52 The estimated mass was 3 MDa.

• l. 74 reference 9 is important, although that work did not establish nsp3 and nsp4 as the minimum system for the formation of coronaviral DMVs. Important references in this regard are PMID: 29162711 (MERS-CoV, SARS-CoV) and PMID: 34907161 (SARS-CoV-2).

• In l. 155, reference 10, did the authors mean to (also) cite PMID: 24928045? In any case, none of these studies demonstrated the presence of pore complexes as stated in the sentence, as they are not visible in conventional EM samples.

Referee #3 (Remarks to the Author):

The authors present a detailed structure of the SARS-CoV-2 double membrane vesicle pore – the gateway to the viral replication factory. Related structures are formed by many positive stranded RNA viruses. Understanding these structures will be central to understanding virus replication. The work is a very substantial advance in our understanding of double membrane pores. It has been well-executed and well-presented.

Although the functional analysis of the structure is minimal, limited to mutation of the positively charged constriction, in my opinion the structure alone will be of broad interest.

I have only minor suggestions for improving the manuscript before publication:

Please include further data to illustrate the confidence in model building in different regions of the structure. For example: linear schematic of the domain architecture clearly marked with which regions are rigid-body fits, which are refined from alpha fold models, which are built, which are not resolved etc; a per-residue Q-score plot; a plot of local resolution onto linear domain architecture.

Please report how many pores are present per DMV.

The methods section describes 4746 tilt series, the table describes 5170 tilt series. Please correct this apparent inconsistency?

The comparison to the nuclear pore is interesting, but the authors should be careful not to stretch the analogy too far.

I suggest not to include the 4.2 Å resolution statement in the abstract since this refers only to the core pore.

Author Rebuttals to Initial Comments:

Referees' comments:

Referee #1 (Remarks to the Author):

Huang et al. present the cryo-electron tomography (cryo-ET)-based structure of the protein pore that was previously found to form in double-membrane vesicles (DMVs) of the SARS-CoV-2. The authors reconstituted DMVs and pores in cells transfected with a fusion of Nsp3 and Nsp4 proteins, which build up the pore, purified the DMVs, collected a large amount of cryo-ET data, and obtained cryo-ET maps at local resolutions ranging from 3.7Å to 7.1Å. Then, they built a structural model based on the maps. They used the models to explain how the pore is built up, how the pore for RNA translocation might be formed, and what might be critical domains and residues for pore stability. Based on the model, they also predicted residues important for RNA translocation and confirmed that using recombinant viruses.

Overall, this is an impressive work in the methodology and results, and has the potential to be a seminal paper in the SARS-CoV-2 and cryo-ET fields. The pore has been identified before, but the previous cryo-ET maps were of very low resolution, and at most, partial and approximate structural models could be proposed (Wolff, 2020; Zimmermann, 2023). The manuscript reads very well, and the figures are clear. The structure is compared to the prior data and pores of other viruses. The structure is fascinating in how the rings of the pore are assembled, how they interact with the membrane, and how the symmetry changes along the axis of the pore. While the comparison to the nuclear pore complex may seem tangential, it offers an interesting perspective for understanding the functional dynamics of double-membrane-spanning pores.

We thank the reviewer's positive comments.

Major comment:
In its current form, the manuscript does not allow for assessing the quality of the structural model, even though a very well-prepared set of cryo-ET maps, local resolution maps, and structures have been provided in the additional data for review. I am aware that many publications do not include such an assessment, but in the opinion of this reviewer, this is necessary.

We thank the reviewer's critical assessment of the model building procedure and have provided the following information: the quality of starting Alphafold model, local quality of model fits to the density maps, overfit assessment and detailed description of modelling procedures, as described below.

The following information needs to be provided:
- Local quality of fits to the cryo-ET maps. Several tools are available for that, such as Q-scores (https://www.nature.com/articles/s41592-020-0731-1), SMOC (https://www.ncbi.nlm.nih.gov/pmc/articles/PMC4854230/), and DAQ (https://github.com/kiharalab/DAQ). The high-resolution regions should be checked for sequence registers using tools like checkMySequence (https://pubmed.ncbi.nlm.nih.gov/35775980/) to have a more quantitative assessment than the visual Extended Data Fig. 6. The authors could use tools as above and provide figures with the scores mapped to the structural model.

We have provided the measurement of local quality of fits to the cryo-ET maps calculated by MapQ and reported the Q-scores of all the models (Figure R1, Extended Data Fig. 6b and Supplementary Fig. 6). The corresponding methods and references are described in Methods section. The high-resolution regions, focusing on the transmembrane helices of both nsp3 and nsp4, have been checked for sequence registers using checkMySequence, which did not reveal potential out-of-register issue.

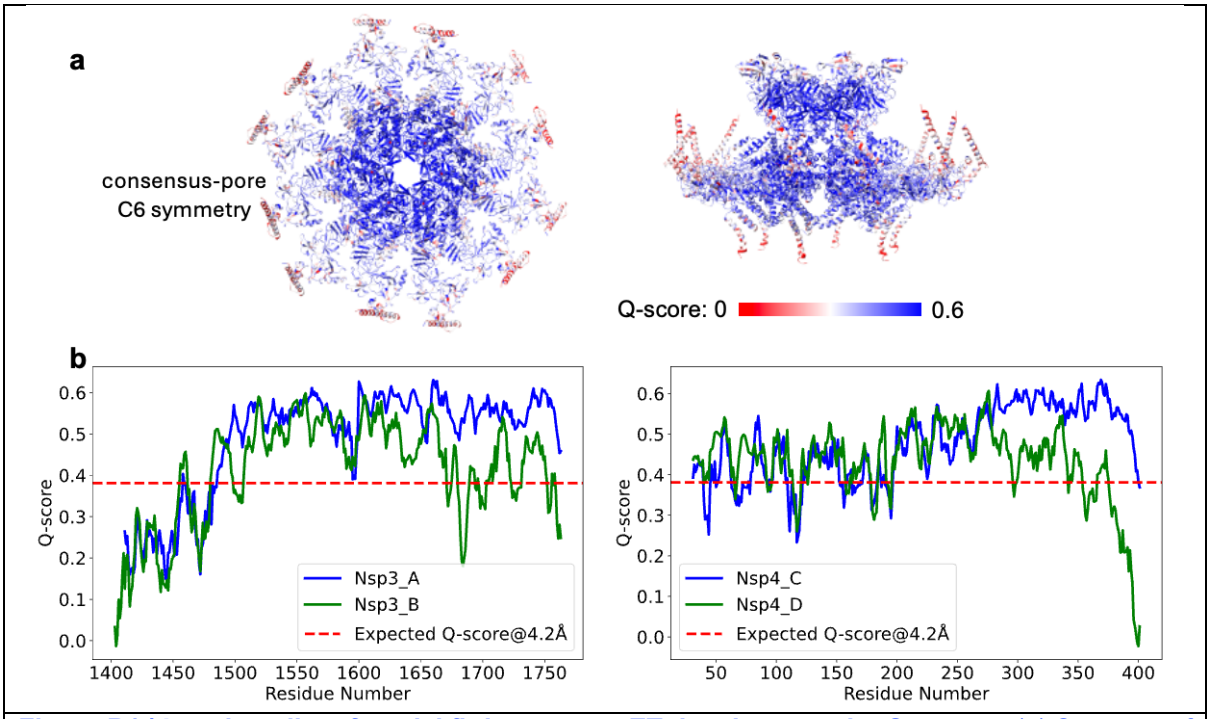

Figure R1 | Local quality of model fitting to cryo-ET density maps by Q-scores. (**a**) Structure of the C6 symmetrized consensus-pore in two orthogonal views, colored by per-residue Q-scores from red to blue (low Q-score to high Q-score). (**b**) Q-score plot of nsp3 and nsp4 chains in the asymmetric unit. The expected Q-score at 4.2 Å resolution is shown as dashed lines. The 5-residue average of Q-scores is plotted here. The Q-score for other models are included in the Supplementary Fig. 6.

- More detailed explanation of the modeling procedure. Currently, it is not possible to understand which regions were modeled de novo, which based on the AlphaFold models. The membrane helices seemed to be done denovo, but were the initial helices taken from AlphaFold or traced manually in Coot? Also, were the Nsp3 and Nsp4 domains modeled with AlphaFold as monomers or as subcomplexes? Which regions were refined in Coot/ISOLDE, and which were kept rigid? Which of the multiple maps obtained were used for building the models?

We apologize for the insufficient description of modelling procedure. We used the Alphafold models as the initial models to build the structure. The nsp3-4 ectodomains were predicted as a complex, as well as the Mac2-3_NAB domains. Other domains were predicted individually (as monomers) or extracted from the predicted full-length models. The individual domains and the two predicted complexes (nsp3-4 ectodomain complex, and the Mac2-3_NAB) were manually fit into the density map by rigid-body docking. The central transmembrane regions shows the highest resolution (<4 Å), which allows manual model refinement in Coot from the predicted models. All the models were subject to ISOLDE refinement and finally refined for their atomic displacement parameters (b-factors) in phenix_refine.

We used the C6 consensus-pore map (which shows the highest resolution) as the starting map to generate the asymmetric unit (ASU). The ASU was then used to fit into the C3 symmetrized consensus-pore map, adding the nsp4-CTD. The ASU from the C6 consensus-pore was then used to build the full-pore map, with additional docking of other domains such as DPUP-Ubl2-PLpro, and Mac2-3_NAB. The final models were refined in ISOLDE and phenix_refine as above.

We have now included a detailed description of the modelling procedure in Methods (*Model building and validation*) and presented a summary of modelling methods for each region in the updated Extended Data Fig. 6a.

- Assessment of overfitting. Several regions of the cryo-ET map have only medium resolution in which side chains are not visible. Placing and refining AlphaFold models in those regions with COOT/ISOLDE may lead to distortions of the starting models and overfitting to the map. To let the reader assess the overfitting, the final model needs to be compared to the starting partial models. This could be done by using figures with side-by-side comparisons, and, ideally, mapping LDTT scores (https://www.ncbi.nlm.nih.gov/pmc/articles/PMC3799472/) on the final model, or plotting per-residue LDDT and local resolution of the cryo-ET map side by side (in case of overfitting, low local resolution regions would coincide with low LDDT).

We thank the reviewer's suggestions to assess the potential overfitting issue and conducted the assessment with the proposed method. We compared the refined models with the starting Alphafold models and mapped the per-residue LDDT to the refined models. Our analysis reveals minimal overfitting issue (Figure R2). The analysis is included in the Supplementary Fig. 7.

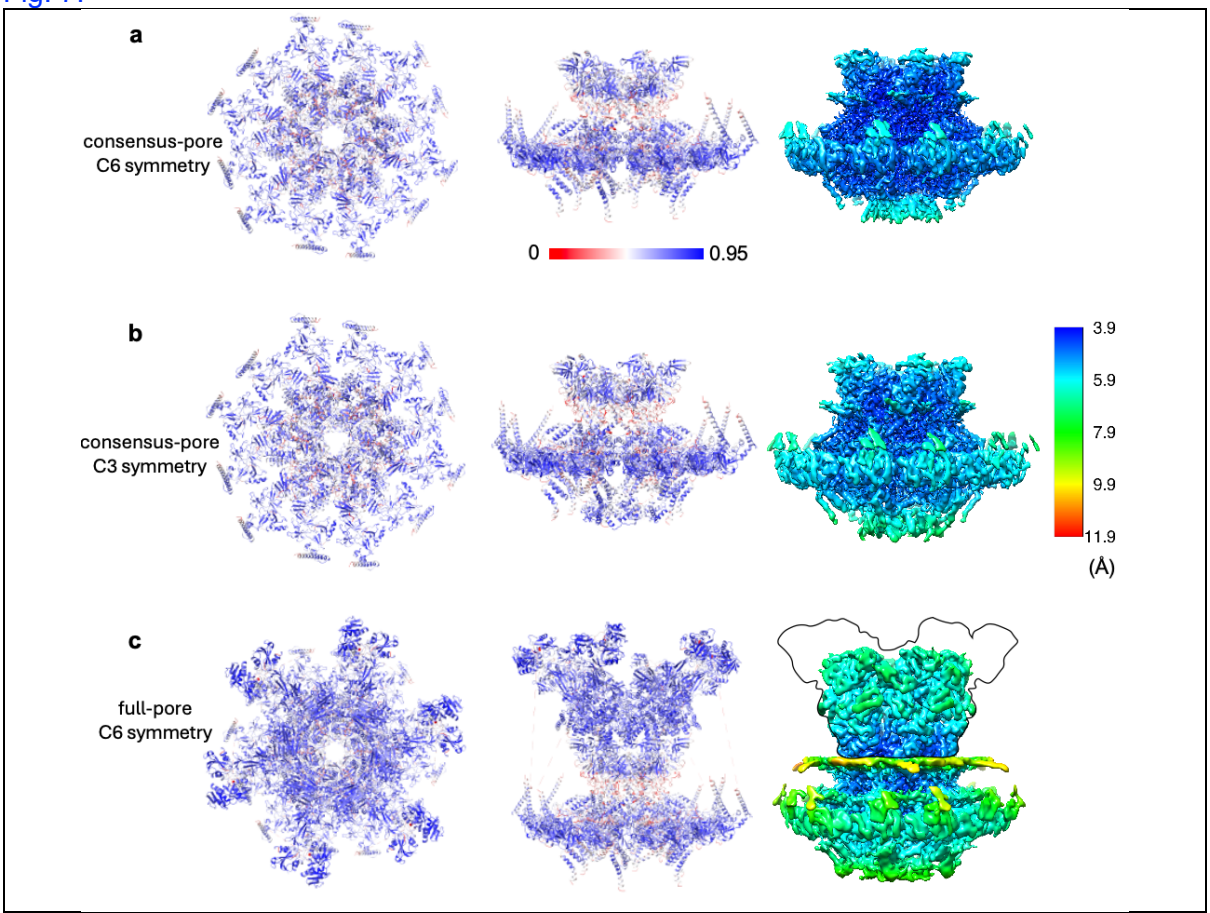

Figure R2 | Assessment of model overfitting by LDDT scores. Two orthogonal views of the six-fold symmetrized consensus-pore (**a**), three-fold symmetrized consensus-pore (**b**) and C6 symmetrized full-pore (**c**), colored by LDDT, which are compared with their corresponding local-resolution estimation maps. The LDDT score was calculated by comparing the refined model with their Alphafold predicted models in Supplementary Information using the online server (https://swissmodel.expasy.org/assess). The models are presented with the calculated LDDT scores colored from red to blue (0-0.95). The low LDDT regions do not match with the local resolution regions, indicating minimal overfitting issues.

- Quality assessment of the starting AlphaFold models. AlphaFold models always come with predicted quality scores, both global and local. These need to be shown. Global pTM and ipTM (if any Nsp3-Nsp4 complexes were modeled) scores should be reported in a table.

Models colored by the local pLDDT score should be used. PAE plots should be shown, regardless of whether Nsp3 and Nsp4 were modeled individually or together.

The AlphaFold models which is colored by pLDDT score and corresponding PAE plots are presented in the Supplementary Fig.2-5 for nsp3 (417-1945), full-length nsp4, nsp3-4 ectodomains and Mac2-3_NAB (corresponding to the tip of the prong). An example of nsp3 (417-1945) is presented here (Figure R3).

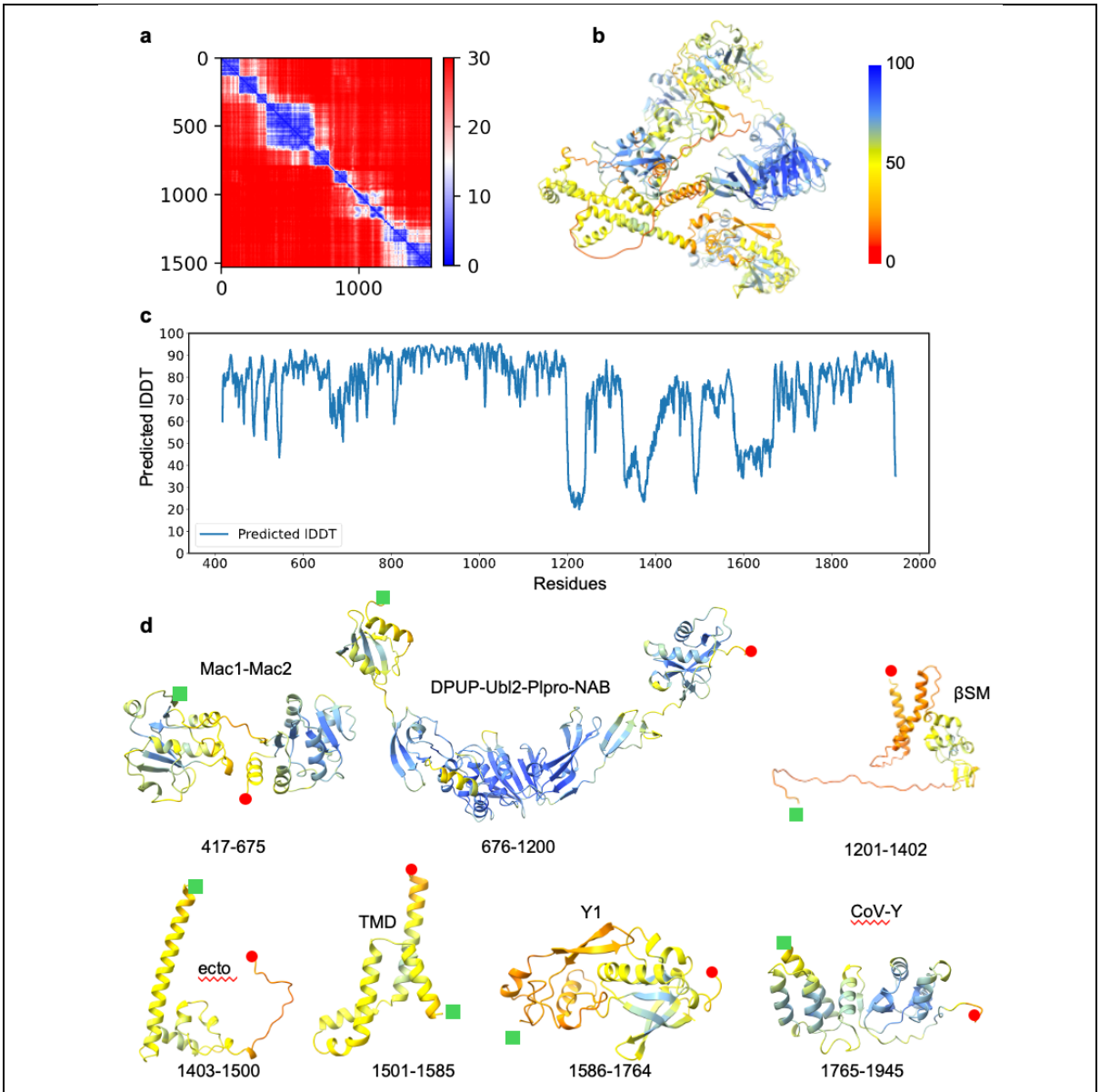

Figure R3 | Alphafold prediction of nsp3 (417-1945). (**a**) Predicted Aligned Error (PAE) plot, showing regions of high confidence (dark blue) and low confidence (red). (**b**) Predicted structure of nsp3(417-1945) colored by pLDDT from 0 to 100 (red to blue). (**c**) Per-residue plot of pLDDT (predicted local distance difference test) scores. (**d**) Domain structures of nsp3(417-1945) colored by pLDDT. The green square and red dot represent the N-terminus and C-terminus of domains, respectively.

- Explanation of: If the model was built by fitting individual domains of Nsp3 and Nsp4 manually, how the interfaces between the domains were refined, and how were the clashes removed? Note that shifting side chains or a backbone with ISOLDE at low resolution to remove clashes may lead to artificial distortions and, thus, incorrect models. Even if that was the case, and

authors want to keep it at that precision, this needs to be reported and would also be clear to the reader when the above overfitting measures are provided.

The model was built by fitting individual domains of nsp3 and nsp4 manually and refined by ISODLE, prior to b-factor refinement using phenix_refine. The clashed residues were reported by phenix_refine and manually checked in Coot. The modelling procedure has been described in detail in Methods (Model building and validation).

Please note that Extended Data Table 1 is necessary to report but does not provide information for addressing the above points. It only reports on the geometrical quality of the structures, which does not exclude overfitting to maps or deviations from the starting structures.

We have now included the details of Alphafold prediction, Q-scores, overfitting assessment in the Extended Data Fig. 6 and supplementary information for all the three models.

Minor comments:
- Indicate the prongs in Figure 1 to clarify their identification for the reader.
The prongs are now indicated in Figure 1, which refer to the nsp3-NTD region (Mac2-3_Ubl2_PLpro_NAB).

- Page 2, lines 63-63: “Our structure reveals an unexpected stoichiometry” – it should be explained why the revealed stoichiometry was “unexpected”.

The nsp3-4 complex was expected to contain 6 copies of nsp3. The previously-reported MHV DMV pore complex display an overall six-fold symmetry, and the estimated molecular weight from the low-resolution density indicates a possible existence of 6 nsp3 in the crown region (Wolf et al, Science, 2020). In contrast and unexpectedly, we identified 12 nsp3 constituting the 6-fold symmetry structure. We added a brief description to indicate this unexpected observation in L65-66: “Our structure reveals an unexpected stoichiometry of coronavirus DMV pore complex constituted by twelve copies each of nsp3 and nsp4, instead of six copies of nsp3 proposed previously, and shows that the…”.

- The Nsp3-4 has been expressed as a tandem polypeptide. Could the authors elaborate in the manuscript why they think this does not change the structure of the pore?

The non-structural proteins in coronavirus are produced as two polypeptides naturally, pp1a and pp1b due to frameshift, which are subsequently proteolytically processed by two viral proteases (PLpro inside nsp3, and Mpro (nsp5)) to generate mature nsps. In the case of nsp3-4 tandem construct, the cleavage between nsp3 and nsp4 is conducted by the PL^{pro} domain within nsp3. Therefore the expression of nsp3-4 tandem will generate mature nsp3 and nsp4 proteins. The same tandem constructs have been used for previous studies to understand the DMV formation by nsp3 and nsp4 (Zimmermann et al, Nature Comm 2023; Oudshoorn et al, mBio 2017). We included the rationale in the main text L75-77: “We therefore expressed the SARS-CoV-2 nsp3-4 tandem polypeptide in HEK 293F cells, which is proteolytically processed into nsp3 and nsp4 by the Papain-like protease (PL^{pro}) within nsp3, to generate DMVs.”

- In Figure 3f, the coloring does not seem to correspond to the other panels; perhaps it could be made consistent for better orienteering.
Figure 3f has the same color scheme as other panels in Fig. 3 - the individual chains were colored differently. However, the original Fig. 3g used the color scheme of Fig. 2a – the domains were colored differently within the same protein, which may have caused confusion. To be consistent within Fig. 3, we have changed the Fig. 3g to match other panels within Fig. 3.

- ISOLDE is not listed in the Reporting Summary
We have now included ISOLDE and other software packages (such as those used for model validations) into the Reporting summary.

- It would be highly appreciated if the raw tilt series were deposited in the EMPIAR database.
The motion corrected 4635 tilt-series and alignment files have been deposited into EMPIAR with the session code: EMPIAR-12038.

- What the B-factor values in the provided PDB files correspond to?
The B-factors in the PDB files are ADP b-factors produced by phenix_refine. We used phenix_refine after ISOLDE and Coot refinement, allowing rigid-body and ADP b-factor refinement.

Referee #2 (Remarks to the Author):

In infected cells, coronaviruses induce an elaborate network of modified host (double) membranes, of which double-membrane vesicles (DMVs) have been identified as the central hub for viral RNA synthesis. Specific membrane-spanning coronavirus replicase subunits (nsp3, nsp4 and nsp6) have been implicated in the formation and structure of DMVs, which – a couple of years ago - were found to contain membrane-spanning pores that are now thought to play a critical role by enabling the export of viral RNA produced inside the DMVs to the cytosol for translation and encapsidation into new virions.

This exciting study reports sub-nm structures of the pore complex spanning the DMVs that are induced following the expression of the coronavirus nonstructural proteins nsp3 and nsp4. Affinity purification of these DMVs, cryotomography and subtomogram averaging provided several density maps of the DMV-spanning complexes. Using pre-existing domain X-ray structures and AlphaFold, the authors construct structural models offering unprecedented insight into the core architecture of these pores and revealing them as made of 12 copies of each nsp3 and nsp4 organized in stacking hexameric rings. The structure suggests novel hypotheses on pore formation and function, and additional mutagenesis experiments included in this study align with these hypotheses. While the question of whether the pore complex reported here is identical to that formed in DMVs in infected cells remains open, this work represents a major step forward to understanding the structural basis of the DMV-spanning pore complexes.

We appreciate the reviewer's positive comments.

While the significance of this study is undeniable, there are some issues that require attention, particularly regarding unresolved masses in the structures:

• The primary concern revolves around the absent masses in both nsp3 and nsp4 across all the structures. Even the complex the authors name "full pore complex" is solved as nsp3L:nsp3S:ns4L:nsp4S (6:6:6:6), with nsp3S lacking the entire N-terminal cytosolic domain, which represents approximately 50% of the total nsp3 mass (~100 kDa). Even larger parts of the proteins are missing in the smaller reported structures ("consensus pore" and "extended pore"). The lack of clarity surrounding this issue is compounded by the complete absence of an explanation for the underlying reasons. Potential explanations may include:

(1) Structural flexibility of these domains, which may result in missing masses in the averaged structures. However, these masses probably are discernable in the individual complexes within the tomograms. Therefore, the fact that individual small pores ("consensus pores") are pointed out in the raw data in Fig. 1a seems to exclude this hypothesis. Yet, the figure is too small, and I propose that a series of individual pore galleries showcasing the three different

types (full pore, extended pore, consensus pore) is presented to better assess this point. In a similar vein, the extended pore structure, omitted from Fig 1a, is it a somewhat artificial product of image processing or does it represent a genuine entity in the DMVs?

The unresolvable mass in the full-pore complex is around 1.2 MDa (nsp3S has ~1400 AAs unresolved whereas nsp3L has ~400 AAs unresolved, each with 6 copies). However, Alphafold prediction indicates that nsp3-NTDs is composed of a series of small domains without strong self-interaction among its domains, which makes it challenging to be resolved directly from the raw tomograms. Furthermore, the purified DMVs tend to cluster together on the cryo-EM grids (Extended Data Fig. 1d), and the background of the tomogram make it difficult to unambiguously judge whether the densities close to the pore complex are nsp3-NTDs. Nevertheless, from the raw tomograms we can identify nsp3-4 complexes with different heights. We have modified Fig. 1a to make it easier for the reader to visualize them. A gallery of more individual pores at different heights are included in the updated Extended Data Fig. 1e.

We reason that the structural flexibility contributes to the unresolved mass in the pore complex:

1) The previous *in situ* tomography work using a similar construct shows no degradation of nsp3 and nsp4 (Zimmermann et al. Nature Comm, 2023). Yet, from their *in situ* tomograms (EMD-15925) we can identify pores with various heights, matching the appearance of full-pore and mini-pore (and consensus-pore) (Figure R4). This strongly supports that the crown region has an intrinsic flexibility, contributing to the apparent height variation of the complex.

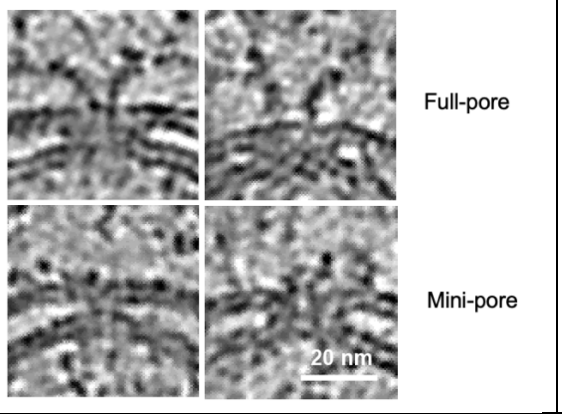

Figure R4 | Full-pore and mini-pore in the *in situ* tomograms from Zimmermann et al Nature Comm, 2023. The pores were extracted from the EMD-15925.

2) Consistently, our full-pore complex structure reveals the stacking of nsp3-NTD (Mac2-NAB) onto the top of upper base: the interaction is mediated by the PLpro with CoV-Y domains (Fig. 2f). The upper base formed by 12 copies of nsp3-CTD interact with 6 copies of nsp3-NTD, leaving no space for the other 6 nsp3-NTDs to engage with the complex in the same interface. So these additional 6 copies of nsp3-NTD are more likely flexible around the pore complex.

Subtomogram averaging and classification revealed three major classes: mini-pore, extended-pore and full-length-pore, varying in the height of cytoplasmic regions (Extended Data Fig. 2e). The major difference between mini-pore and extended-pore lie in the CoV-Y domains in the extreme C-terminus of nsp3, which is ~240 kDa (12 copies of CoV-Y domain, ~20 kDa each). Such differences are generally expected to be resolvable by subtomogram classification methods. Therefore, the observed structural variation between mini-pore and extended-pore should represent two genuine entities, unlikely due to image processing artifact. However, whether this is due to degradation or flexibility remains to be explored.

(2) The actual existence of shorter forms of nsp3. (The Western blots in Extended data figure

1 may suggest this option?). If so, is this biologically significant or merely a result of degradation during purification? How does it align with the previous knowledge about nsp3? Considering the nsp3-4 expression system used, could this be a product of splicing, which would not be relevant in the context of cytosolic replication during viral infection?

As the reviewer pointed out, the western blots in Extended Data Fig. 1a suggest degradation of nsp3 after DMV isolation, which could be the major reasons to lead to the prevalence of shorter forms of nsp3-4 complex in our dataset, although protease inhibitors have been included during DMV isolation. By contrast, we note that the *in situ* nsp3-4 pore complexes are mostly full-pore form (re-examined using EMD-15925), in contrast with the prevalence of mini-pores in our isolated DMVs. This suggests a potential degradation or damage of pore complex during DMV isolation. We also speculate that our DMV isolation protocol may somewhat damage the pore complex: the Twinstrep-GFP tag is localized in the N-terminal of nsp3, and when the whole DMV is anchored to the streptavidin resin by the Twinstrep tag, it is possible that the pulling-force may partially dissociate the nsp3-NTD from the nsp3-4 complex on DMV, especially during resin washing steps.

We use a codon-optimized tandem construct in this work which should not generate splicing variant during protein expression in HEK293T.

Functionally, the shorter form is sufficient to form DMV and assemble into a mini-pore complex, as revealed in the cellular tomography study reported previously: nsp3-4(ΔUbl1-Ubl2) can form DMV and pore complex (Zimmermann et al. Nature Comm, 2023), structurally similar to our mini-pore reported here (Extended Data Fig. 7g). However, these shorter forms, if exist during virus infection, is unlikely functional due to absence of critical domains such as (Ubl1 and Macrodomains), deletion of which abrogates viral replication. On the other hand, these short forms of DMV pore complex may represent the intermediate states towards the full-pore assembly, or even play a regulatory role in pore activity. Further *in situ* investigation by cryo-electron tomography in the virus-infected cells is warranted to resolve this issue.

In conclusion, we suggest that the invisible structures are attributed to both structural flexibility and sample degradation during DMV isolation. Further optimization of DMV isolation protocols might help to alleviate the degradation issue, to better resolve the structure and function of cytoplasmic crown regions. We included the following discussions in the main text: “We identified three major conformations of nsp3-4 pore complex in our dataset, with the mini-pore complex as the prevalent species (**Extended Data Fig. 2e**). In contrast, the same complex *in situ* was found as a full-pore complex[13], with a minor population of mini-pores. Therefore, the heterogeneity of nsp3-4 complexes *in vitro* could be attributed to both conformational flexibility and sample degradation during DMV isolation, with the latter likely being the primary factor. Nonetheless, considering that the nsp3-NTD is stacked onto the upper base of pore complex by interacting with CoV-Y ring in the full-pore, it is also possible that the shorter forms represent the intermediate states towards full-pore assembly.”

• Another critical (but small) mass not resolved or mentioned is the hydrophobic N-terminal domain of nsp4: residues 1-30, with residues 10-30 being a predicted TM domain, and a domain that is liberated by the nsp3/4 cleavage, which must occur on the cytosolic side of the membrane. It remains entirely unclear why this region has not be resolved, warranting attention in the article. Its omission in Fig.2a renders the figure confusing. Given that nsp3-4 are expressed as a single polypeptide, the N-terminal domain of nsp4 must (at least initially) be cytosolic, with the nsp3-4 junction accessible to the PLpro domain of nsp3 for cleavage.

We agree that the N-terminal residues should be located prior to the nsp4-ectodomain, which should structurally locate to the very peripheral site of the complex. However, the local resolution and resolvability of the map does not allow confident assignment of this helix. To avoid confusion, we have now included this TM1 in the schematics of nsp4 (Fig. 2a, Fig. 3g,

Extended Data Fig. 8c). We remain excluding this helix in the structural models presented in this work. Further work is required to improve the local resolution to model the TM1.

• Notice that, without this pivotal N-terminal nsp4 segment that should cross the membrane, the luminal orientation of the nsp4 ecto domain would not be possible, and therefore it is critical for the proposed model of pore formation through cis-oligomerization of the nsp3 end nsp4 ectodomains (l. 208-215) and the membrane zippering through trans-interactions. I strongly encourage the authors to include a schematic illustration of this model as an Extended figure and in the context of DMV formation, as this would be extremely informative. If space restrictions apply, this figure could substitute Extended Data Figure 10, which, in my view, conveys little information.

We strongly agree with the reviewer's suggestion about the nsp4-TM1 and provide a schematic illustration of the proposed model for membrane reorganization and pore formation. We have included the first helix of nsp4 in the schematic to illustrate the potential pathway in Extended Data Fig. 8c (Figure R5). The original Extended Data Figure 10 was removed as suggested.

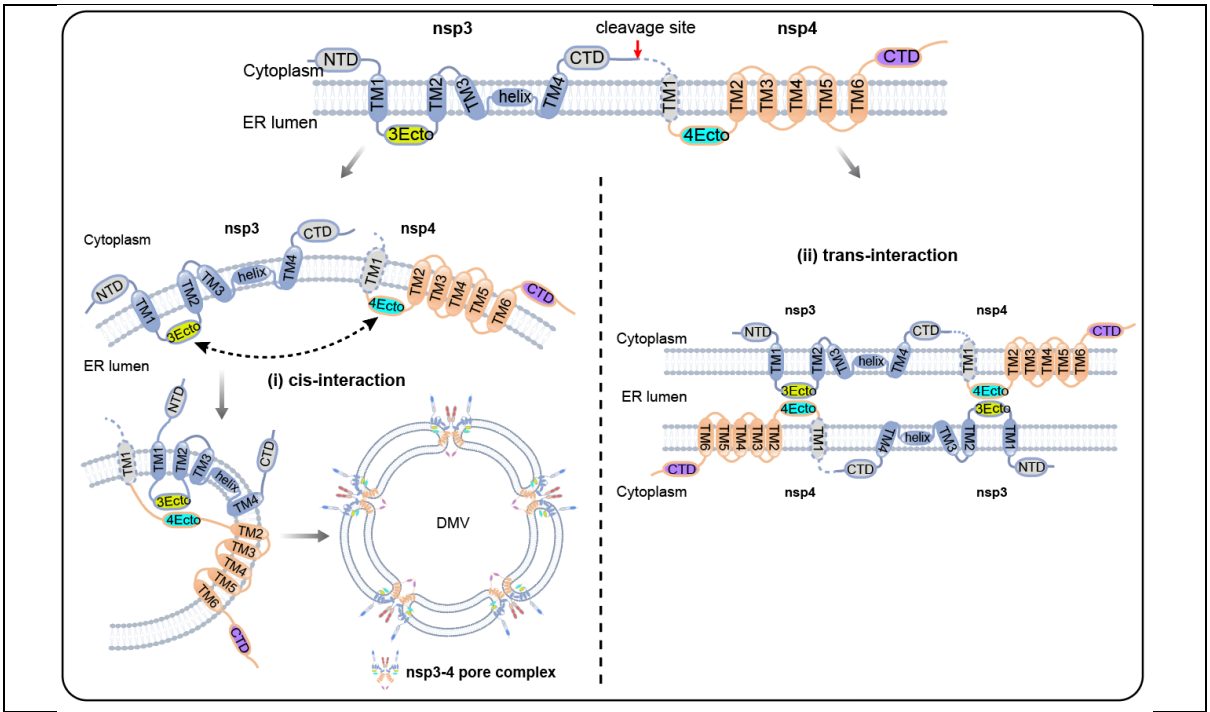

Figure R5 | Schematics of DMV formation by the wild-type nsp3-4 and membrane zippering by the cleavage-deficient mutant. Cis-interaction of nsp3 and nsp4 ectodomains leads to local high curvature and subsequent DMV formation whereas trans-interaction results in membrane zippering. Red arrows show PL^{pro} cleavage site between nsp3 and nsp4.

• Note also that the existence of this additional nsp4 TM segment has implications for the nomenclature of the nsp4 TM helices resolved, which would be TM2-TM6 rather than TM1-TM5. It would seem important not to create nomenclature confusion in this (potentially) seminal publication, which will likely be a reference point for many future studies. Likewise, the reason to call TM4 of nsp3 a TM domain is not very clear, as the domain does not seem to be spanning the membrane (Fig. 2a). It should be considered to name it differently as many will assume that the number of TM domains (even or odd) automatically defines whether the N- and C- termini of nsp3 are on the same or opposite sides of the membrane.

We thank the reviewer's correction and have change the nomenclature throughout the manuscript to avoid confusions for readers: (1) rename nsp3-TM4 as "helix" since it does not

pass the membrane bilayer; we refer it as “horizontal helix” in the main text as it lies almost horizontal with respect to membrane surface; (2) add TM1 of nsp4 (residues 10-31) into schematics and rename the rest of the helices as TM2-TM6 accordingly.

• Another puzzling aspect of the structure is the considerable distance between the NAB and TM1 regions of nsp3L, situated essentially on opposite sides of the pore (see, for example, Fig. 2f), while only separated in the sequence by the βSM domain. It remains unclear how this unresolved domain could bridge this distance, as this is not addressed in the article.

We thank the reviewer to raise this interesting point. The distance between NAB and TM1 of nsp3L is 11 nm, measured from the structure. Between NAB and TM1 region, there are 215 amino acid residues which is predicted to contain two helices, a βSM domain and a long disordered region (Figure R6). The distance of the disordered region (residues 1199-1241) can span as long as 14 nm (0.35 nm between two residues x 40 residues = 14 nm). Adding the additional βSM domain (which is 4 nm in length), this unresolved region is therefore sufficiently long to link NAB and nsp3L-TM1. Further study to improve the local resolution of the peripheral region will be required to resolve more details between NAB and nsp3L-TM1.

We explained this possibility in the Methods section: “The unresolved region between NAB and nsp3-TM1 consists of >200 amino acid residues, which is predicted to contain two helices, a βSM domain and a long-disordered loop (Supplementary Fig. 2). The distance of the disordered loop (residues 1199-1241) can span as long as 14 nm, and with the additional βSM domain (which is 4 nm in length), this unresolved region is sufficiently long to link NAB and nsp3L-TM1.”

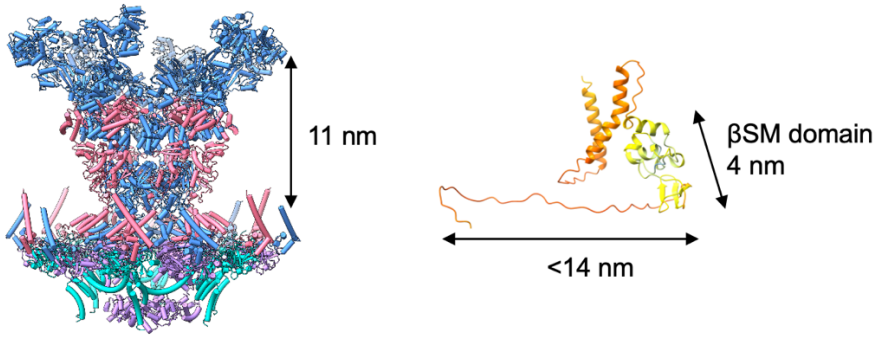

Figure R6 | The unresolved region between NAB and nsp3L-TM1. The alphafold predicted model of the unresolved region between NAB and nsp3L-TM1 is shown on the right, colored by alphafold prediction confidence scores from low to high (red to blue). The distances between NAB and nsp3L-TM1 and the length of the partially disordered region are indicated.

Mutagenesis experiments:

• Negatively charged mutations introduced in the ectodomain of nsp3 seem to impede or reduce the interaction with nsp4, nicely supporting the author’s model (Fig. 3i). However, and despite the absence of mutations in nsp4, the input gel shows poor expression and double bands for nsp4, a factor that could potentially affect the main claim.

In agreement with the reviewer, we noticed that nsp4 level is somehow affected in the nsp3-4 tandem mutant constructs, whereas the level of nsp3 per se as not affected. To address this issue, we have attempted to co-express various nsp3 constructs with wild-type nsp4 instead of nsp3-4 tandem construct. Surprisingly, nsp4 could only be detected in the pull-down experiment when wild-type nsp3 is co-expressed (Figure R7). This suggests that nsp4 itself may be unstable and could only become stable when its interaction with nsp3 is maintained (as in the wild-type and nsp3-V1458A/L1480A mutant). We further conducted cryo-cellular

tomography for the wild-type and two mutants to observe the effect of these interactions in situ (see below).

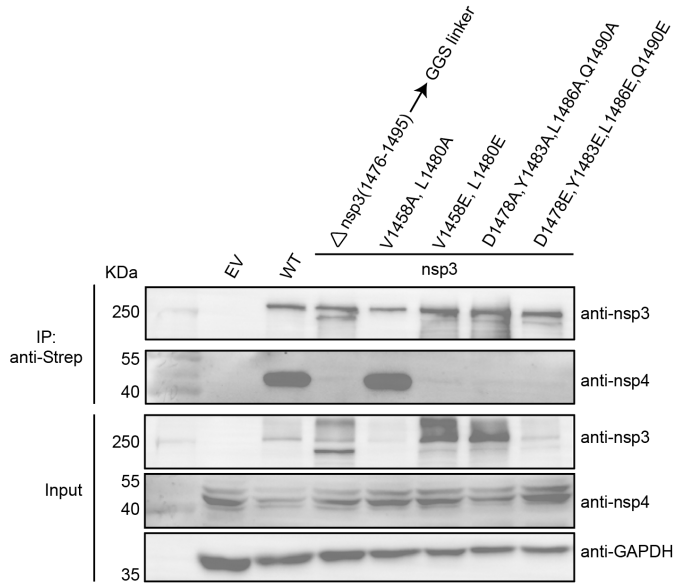

Figure R7 | Co-immunoprecipitation assay of nsp3 and nsp4. The wild-type or mutant nsp3 were co-transfected with wild-type nsp4 (equal amount) into HEK 293T cells. Two days after transfection, the cells were harvested and subject to co-immunoprecipitation assay in the same way as described in the Methods (*Co-immunoprecipitation and Western blot analysis).* Unexpectedly nsp4 could not detected in the cell lysate (only shown as none-specific bands in the input), but can be co-immunoprecipitated in the WT and V1458A/L1480A.

• The second set of mutagenesis experiments summarized in Extended Data Fig. 9 align with the suggested notion that the charged residues inside the channel of the structure are critical for viral replication. Importantly, however, the rescue experiment with recombinant mutant viruses in panel b appears to lack a positive control (wt), which would be critical to exclude issues with the experimental setup.

We thank the reviewers comments and have included both the positive control (wt) and more mutants in the virus rescue experiment, as shown in the updated Fig. 4e. We have convincingly shown that the positive-charged substitution in the central pore (nsp4-R306K) does not change virus replication significantly, whereas even a single negative-charged and neutralization substitution in the central pore abolishes virus replication. These results are elaborated in the main text.

• Given the potential influence of unrelated factors on the outcomes of both sets of mutagenesis experiments, it would be important to assess the structures formed (DMVs? paired membranes? pores?) in one or two selected mutants using the expression system. This step would significantly contribute to strengthen the conclusions.

We have performed two different sets of experiments for the five selected mutants and wild-type, to better understand the interfaces.

For the nsp3-4 ectodomain interface mutants that may affect DMV formation, we conducted cryo-FIB milling of the transfected VeroE6 cell by the wild-type nsp3-4 and mutants (Figure R8). Due to the low transfection efficiency of VeroE6 cell, we performed flow cytometry after transfection and seeded the GPF-nsp3-postive cells onto cryo-EM grid. By cellular cryo-ET, we observed that 1/6 cells in double mutant (nsp3-V1458E/L1480E, middle) display clustered DMVs, whereas only a few DMV-like structures can be sparsely identified in the quadruple mutant (nsp3-D1478E/Y1483E/L1486E/Q1490E, right). We observed some convoluted

membrane structures with unknown species in both mutants. In contrast, 2/6 of the wild-type transfected cells revealed clear clustered DMVs. These results indicate that DMV formation in these two mutations are reduced.

We have included the cellular tomography data as the new Extended Data Fig. 8a-b, and described the results in main text: "To determine whether these negatively charged substitutions affect DMV formation, we conducted *in situ* cryo-ET of transfected VeroE6 cells following cryo-focused ion beam milling. The double mutant (V1458E/L1480E) still revealed clustered DMV structures, whereas the quadruple mutant (D1478E/Y1483E/L1486E/Q1490E) exhibited only convoluted membranes and scarce DMV-like vesicles (**Extended Data Fig. 8a-b**)." The methods related to cellular tomography are included in Methods.

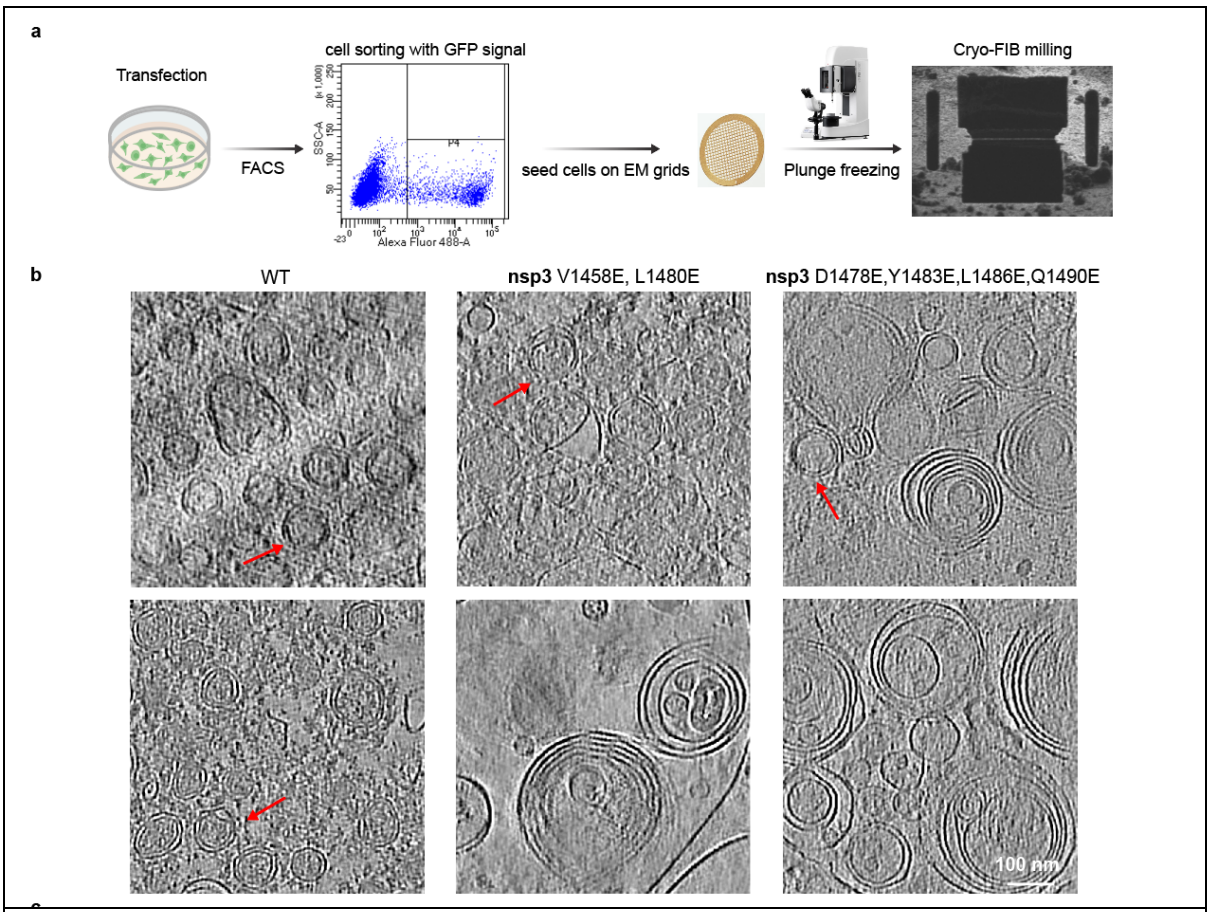

Figure R8. | Cellular cryo-ET of WT and mutant nsp3-4. (**a**) A schematic representation of lamella preparation of VeroE6 cells transfected wild-type and mutants of TwinStrep-GFP-nsp3-4 construct. The transfected VeroE6 were subject to flow-cytometry and the resulting GFP-positive cells were seeded onto cryo-EM grids for the subsequent cryo-FIB and cryo-ET. (**b**) Slices of tomograms of VeroE6 cells transfected with nsp3-4 tandem constructs: wild type nsp3-4 (left), double mutant (nsp3 V1458E/L1480E, middle) and quadruple mutant (nsp3 D1478E/Y1483E/L1486E/Q1490E, right). Red arrows show potential DMVs. Two representative tomogram slices are presented for each construct. Scale bar = 100 nm.

For the central-pore mutations, we have expressed and isolated the DMVs and performed subtomogram averaging of the resulting pore complexes. These pore mutants can still generate similar DMVs (Figure R9). The central Arg residues mutation do not affect pore formation, whereas other two mutants appear to affect the pore structure, as indicated by the blurring of the cytoplasmic crown (nsp3-CTD) and luminal regions (nsp4-CTD) in the two mutants. This demonstrate the pore integrity is essential for virus replication. These results are included in the main text and the updated Extended Data Fig. 10c-d.

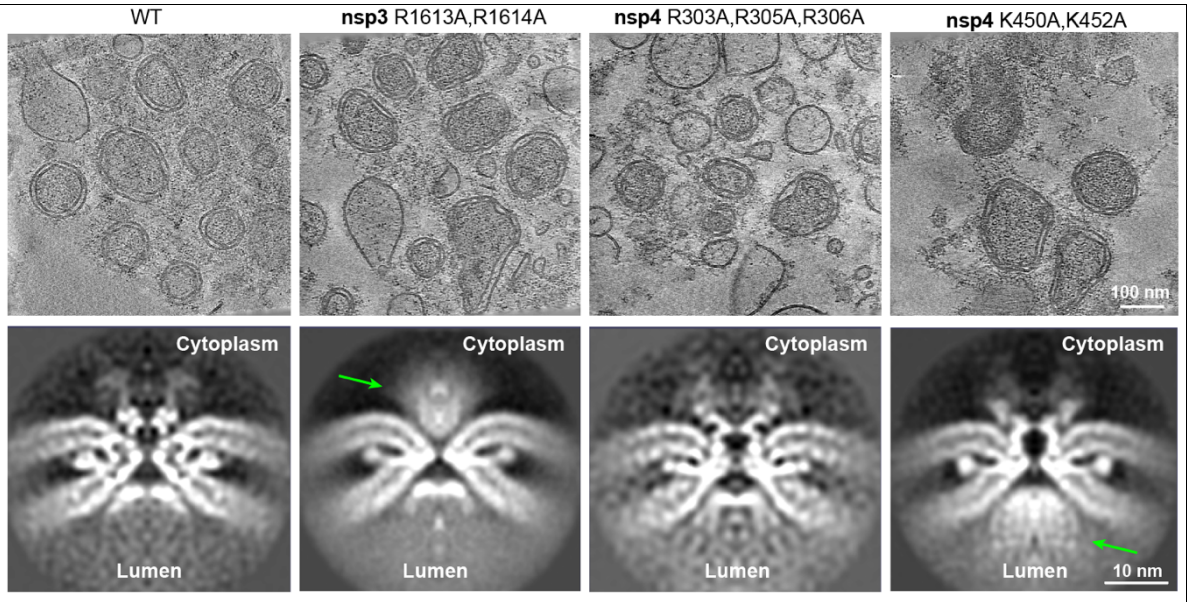

Figure R9 | Characterization of pore mutants by cryo-ET and subtomogram averaging. The representative tomogram slices of purified wild-type and mutant DMVs are shown on the top panel. Scale bar = 100 nm. The bottom panels show the longitudinal cross-sections of the wild-type and mutant nsp3-4 complexes revealed by subtomogram averaging. The number of particles used for subtomogram averaging for each dataset: 1000, 1414, 840 and 842 (from left to right). Green arrows indicate the more blurred densities compared with the wild-type pore. Scale bar = 10 nm.

Others:

• A point not directly addressed in the text is the possible disparities with the pore complexes formed in infection. The lack of e.g. RdRp and RNA synthesis, and the potential consequences should be pointed out to the reader. In this regard, l. 22 in the abstract referring to "SARS-CoV-2 pore complex" is misleading –maybe use nsp3-4 complex, as in the rest of the text.

We have changed to nsp3-4 complex throughout the text to avoid confusion and included the following statement in the main text to acknowledge the possible disparities between nsp3-4 complex and the complete DMV pore complex formed by virus infection in Discussion: "The architecture of our nsp3-4 full-pore complex closely resembles the native authentic DMV pore complex observed during MHV infection in situ. The conformation of nsp3-4 complex without RNA may represent a resting-state of DMV pore during RNA and metabolite transportation. However, due to the absence of RNA synthesis machinery in our minimal DMV system, our nsp3-4 complex may not fully recapitulate the complete functional DMV pore complex during virus infection." Further study of the complete functional DMV is warranted.

• The claim in line 60 should be tempered, as it appears premature; at present, it stands as an exciting and plausible yet hypothetical model. Note that, as indicated in the previous point, there is not RNA in the nsp3-4 protein expression system.

We have attenuated this premature claim to "…we describe the structure of coronavirus DMV pore complex using isolated DMVs formed by minimal viral components (nsp3-4) *in vitro*…"

• L. 249-250. For another betacoronavirus (MHV, mouse hepatitis virus), a nsp4 mutant with a ~100 amino acid C-terminal deletion has been reported to be viable (Sparks et al. 2007, PMID: 17855548), which may argue against this hypothesis.

We thank the reviewer to bring out this work. In the original submission, our mutagenesis results showed a clear evidence of the positively-charged residues in the virus replication. To further substantiate this, we constructed a SARS-CoV-2 BAC-clone deleting nsp4-CTD, which

was found to be not viable as well, in agreement with the nsp4 mutation results (Fig. 4e). The species-dependent variations among the different coronavirus warrants further detailed investigation.

• For the sake of clarity for non-expert readers, the pore complexes in the neck of the spherules that are induced by other viruses, such as nodaviruses or alphaviruses, and which appear in results and figures, should already be mentioned in the introduction.

We have added the following introduction sentences in the introduction section in L43-44: “Similarly, alphavirus (such as Chikungunya virus) and nodavirus induce membrane spherules as replication organelle for viral genome replication, forming a large ring complex at the membrane neck”.

• Please, indicate the transfection efficiency in the purification setup. Was GFP added as a tag to the nsp34 construct to assess this point? Right now, the reason behind its inclusion in the constructs is unclear.

We observe around 60%~70% transfection efficiency of HEK Expi293F cells for DMV expression and purification in our experiment. The GFP tagged in the N-terminus of nsp3 was used to aid the visualization of DMV isolation procedure: the DMV-bound streptavidin resin can be visualized directly during purification. The GFP signal was also used for flow cytometry to obtain the transfected Vero E6 cells for the subsequent cryo-focused ion beam milling and cellular tomography. We included a description of the rationale of the construct design in the Methods: “The presence of EGFP allows the timely assessment of transfected cells and the subsequent DMV isolation procedure.”

• L. 52 The estimated mass was 3 MDa.
Changed to 3 MDa.

• l. 74 reference 9 is important, although that work did not establish nsp3 and nsp4 as the minimum system for the formation of coronaviral DMVs. Important references in this regard are PMID: 29162711 (MERS-CoV, SARS-CoV) and PMID: 34907161 (SARS-CoV-2).

We have cited these two references PMID: 29162711 (MERS-CoV, SARS-CoV) and PMID: 34907161 (SARS-CoV-2).

• In l. 155, reference 10, did the authors mean to (also) cite PMID: 24928045? In any case, none of these studies demonstrated the presence of pore complexes as stated in the sentence, as they are not visible in conventional EM samples.

We added the new reference PMID: 24928045 and removed the “and pore formation” in main text. These studies demonstrated that DMV formation can be achieved with nsp3C and nsp4.

Referee #3 (Remarks to the Author):

The authors present a detailed structure of the SARS-CoV-2 double membrane vesicle pore – the gateway to the viral replication factory. Related structures are formed by many positive stranded RNA viruses. Understanding these structures will be central to understanding virus replication. The work is a very substantial advance in our understanding of double membrane pores. It has been well-executed and well-presented. Although the functional analysis of the structure is minimal, limited to mutation of the positively charged constriction, in my opinion the structure alone will be of broad interest.

We thank the reviewers positive comments and have included more characterization of the mutants using both the nsp3-4 tandem constructs and virus BAC, to further strengthen our major findings in this work.

I have only minor suggestions for improving the manuscript before publication:

Please include further data to illustrate the confidence in model building in different regions of the structure. For example: linear schematic of the domain architecture clearly marked with which regions are rigid-body fits, which are refined from alpha fold models, which are built, which are not resolved etc; a per-residue Q-score plot; a plot of local resolution onto linear domain architecture.

We have provided a detailed description of modelling procedures in Methods, and included a linear schematics of domain architecture colored by the local resolution of domains. The methods that are used to model the structures are labelled to the schematics in the updated Extended Data Fig. 6a. A per-residue Q-score and other validation plots are provided in Extended Data Fig. 6b and Supplementary Fig. 6.

Please report how many pores are present per DMV.

We estimated the number of pores per DMV after 3D classification: “In average, ~5 nsp3-4 complex can be identified from each DMV after 3D classification, which is estimated from a subset of dataset containing 5101 particles from 996 DMVs.” The previous reports observed ~10 pores per DMV. Our calculation based on 3D classification results may under-estimate the real number of pores: to obtain high-resolution pore complex, only the good quality pores were kept for the subsequent subtomogram averaging.

The methods section describes 4746 tilt series, the table describes 5170 tilt series. Please correct this apparent inconsistency?

We apologies for the inconsistency and have corrected the table and methods. We collected 5170 raw tilt-series and used 4635 tilt-series for subsequent subtomogram averaging and classification.

The comparison to the nuclear pore is interesting, but the authors should be careful not to stretch the analogy too far.

We have removed the original Extended Data Fig.10 for the analogy of NPC with nsp3-4 complex.

I suggest not to include the 4.2 Å resolution statement in the abstract since this refers only to the core pore.

We have modified the statement to avoid confusion in the abstract: “we describe the molecular architecture of SARS-CoV-2 nsp3-4 pore complex, as resolved locally up to 3.9 Å resolution by cryo-electron tomography and subtomogram averaging”.

Reviewer Reports on the First Revision:

Referees' comments:

Referee #1 (Remarks to the Author):

Beautiful! My comments regarding the model assessment have been outstandingly addressed, and I will use this paper as an example of how such assessment should be done. I have no further comments.

Referee #2 (Remarks to the Author):

First, I would like to commend the authors on their excellent job in thoroughly addressing the points I previously raised. I only have a few minor remarks on their responses and the revised manuscript. These can be easily addressed and likely do not require further evaluation by this reviewer, except perhaps for the first point in the following list.

• I greatly appreciate the inclusion of the model that is now provided in Extended Data Fig. 8. However, in the wild type case (left part), there is a significant leap in the final step –the transition from the bending of a single membrane following the cis-interactions of the nsp3 and nsp4 ectodomains to the formation of a DMV containing multiple pore complexes. Bridging this gap is challenging, and it would be important to include the author's perspective on this matter. While I agree that the membrane curvature generated by the pore complex could contribute to DMV formation, it seems to me that this alone is not sufficient and that membrane fission events would also be required.

Please note that current models for coronavirus DMV biogenesis postulate that the initial step is the formation of paired membranes, which are observed in cells infected with several coronaviruses (e.g. IBV). In this alternative scenario, pore formation could be a local event occurring within a paired membrane –and not on a single membrane, as indicated in the provided scheme.

Notably, the limited data available on the kinetics of coronavirus replicase polyprotein seems to indicate that the nsp3-nsp4 junction is cleaved rapidly (e.g. PMID 10933699). This would suggest that membrane pairing, as observed in IBV-infected cells, for example, can be mediated by fully cleaved nsp3 and nsp4.

In any case, in the absence of firm experimental evidence, I would agree that there is room for speculation and alternative models. Nonetheless, it would be important to include these alternative possibilities and/or highlight the gaps in our current knowledge within the model presented.

• Mutagenesis experiments: The additional data and explanations provided are very illuminating. Even if the peer review correspondence is included in the publication, it would be helpful to include an explicit remark in the manuscript about the nsp4 instability, as the low nsp4 levels and double bands are quite apparent.

• Regarding the in situ data with the nsp3-4 mutants:
(1) the results seem to indicate that, in some cases, DMVs are formed, although much less abundantly. However, I would be cautious, as cryo-lamellae obtained by FIB-milling represent a miniscule fraction of the cell and are therefore not well suited for quantifications --unless large numbers of lamellae are produced, which is practically unattainable. Consequently, statements like "2/6 cells for the wild-type transfected cells revealed clustered DMVs" (rebuttal) are problematic. Please, consider this when presenting your conclusions in the manuscript.
(2) An important point is whether pore complexes were observed in these DMVs, and this should be clearly indicated.
(3) I would strongly recommend avoiding the use of the term "convoluted membranes" here (l. 201). In the coronavirus field, this term typically refers to a distinct type of double-membrane structure induced by coronaviruses, as described in studies such as Knoops et al. (PMID: 18451981). The structures presented in the figures are entirely different and may simply represent residual bodies of the lysosomal pathway.

Other points:

l. 44 "membrane neck" should be "spherule neck"

l. 67-68. Please revise the phrasing. Reference 7 did not propose that the complex contained only six copies of nsp3. Indeed, the study detected only the six copies of nsp3 on the crown of the complex, which is perhaps unsurprising given the present structure and the presumed flexibility of the NTDs in the second set of nsp3. However, these six copies nsp3 were proposed to form part of a larger complex that should contain additional components, unidentified at the time.

l. 166 six transmembrane helices, not five.

l. 232-233 mentions conservation of these residues across α & β coronaviruses referring to source data in which only conservation plots of β coronaviruses are included.

l. 248. Unfinished sentence: "failed to rescue…" what?

l. 253. Using "cytoplasmic part of the pore complex" and "luminal part of the pore complex" would be more appropriate than "cytoplasmic pore" or "luminal pore". Additionally, replacing "pore" with "pore complex", here and throughout the text may be a better alternative, as "pore" could also refer to just the hollow channel inside the complex.

l. 262. While I acknowledge the similarities, I believe it is important to highlight the striking differences. Specifically, the RdRp and capping functions are integrated into the pore complexes of the spherules induced by noda- and alphaviruses.

l. 280-281. Please rephrase for clarity. I think the authors are referring to the presence of a CTD domain, which is a feature shared by coronaviruses and arteriviruses. However, the arteri- and coronavirus CTD domains are quite different with no sequence conservations. Additionally, the authors should probably exercise caution in extending their conclusion to the entire Nidovirales

order, as the group is rapidly expanding, uncovering unexpected variability in genomes and genome organization (see PMID: 38648214).

l. 432 non-viable instead of inviable.

l. 645 notes 9510% humidity, I assume this is a typo.

Referee #3 (Remarks to the Author):

The authors have satisfactorily addressed my concerns.

Author Rebuttals to First Revision:

Referees' comments:

Referee #1 (Remarks to the Author):

Beautiful! My comments regarding the model assessment have been outstandingly addressed, and I will use this paper as an example of how such assessment should be done. I have no further comments.

We appreciate the reviewer's very positive comments.

Referee #2 (Remarks to the Author):

First, I would like to commend the authors on their excellent job in thoroughly addressing the points I previously raised. I only have a few minor remarks on their responses and the revised manuscript. These can be easily addressed and likely do not require further evaluation by this reviewer, except perhaps for the first point in the following list.

We thank the reviewer's positive comments and have addressed the following issues as below.

• I greatly appreciate the inclusion of the model that is now provided in Extended Data Fig. 8. However, in the wild type case (left part), there is a significant leap in the final step –the transition from the bending of a single membrane following the cis-interactions of the nsp3 and nsp4 ectodomains to the formation of a DMV containing multiple pore complexes. Bridging this gap is challenging, and it would be important to include the author's perspective on this matter. While I agree that the membrane curvature generated by the pore complex could contribute to DMV formation, it seems to me that this alone is not sufficient and that membrane fission events would also be required.

Please note that current models for coronavirus DMV biogenesis postulate that the initial step is the formation of paired membranes, which are observed in cells infected with several coronaviruses (e.g. IBV). In this alternative scenario, pore formation could be a local event occurring within a paired membrane –and not on a single membrane, as indicated in the provided scheme.

Notably, the limited data available on the kinetics of coronavirus replicase polyprotein seems to indicate that the nsp3-nsp4 junction is cleaved rapidly (e.g. PMID 10933699). This would suggest that membrane pairing, as observed in IBV-infected cells, for example, can be mediated by fully cleaved nsp3 and nsp4.

In any case, in the absence of firm experimental evidence, I would agree that there is room for speculation and alternative models. Nonetheless, it would be important to include these alternative possibilities and/or highlight the gaps in our current knowledge within the model presented.

We agree with the reviewer that there is still a significant gap in our model, between single membrane bending to form paired membrane and the final closed DMV formation. However, in the author's view, our model can be reconciled with the current DMV biogenesis model in which the paired membrane is the initial step. In our current model, we propose that the interaction of nsp3 and nsp4 leads to the formation of curved membrane locally from a single membrane, prior to paired membrane formation. Speculatively, the individual DMV pore complex can be formed by the local membrane fusion events occurring at the edge of paired

membrane: Firstly, nsp3 and nsp4 protomers assemble into partial nsp3-4 complex on the edge of paired membrane; Secondly, the addition of more protomers into the partial nsp3-4 complex would then result in a complete pore complex on the paired membrane, with a concurrent local membrane fusion event; Thirdly, the paired membrane sheet is eventually fused to form the closed DMV, potentially again mediated by more nsp3-4 complex or other cellular membrane fusion/fission machinery. This model would be consistent with the previous finding that DMV pore complex were identified in the paired membrane, in addition to the complete closed DMV from the *in situ* cryo-ET study (Zimmermann et al, 2023).

Overall, we propose nsp3-4 pore formation leads to the paired membrane formation; the paired membrane (with DMV pore complexes on it) then acts as an intermediate stage towards the closed DMV formation. However, how these paired membrane are further developed into closed DMV remains mysterious. We do not include the proposed transition step in the model due to the lack of evidence. Further experimental evidences are necessary to validate the model to understand the detailed mechanism of DMV formation, potentially through a time-lapse cellular tomography experiment to visualize the development of paired membrane during DMV formation.

We include a brief statement to indicate the gap in the mechanism of DMV formation: "… for the pore to assemble (Extended Data Fig. 8c). This could further develop into paired membrane sheet with double-membrane-spanning pores stabilizing it, as observed previously in situ. However, how these paired membranes are developed into closed DMV remains unknown and experimental evidence is required to substantiate this hypothesis."

• Mutagenesis experiments: The additional data and explanations provided are very illuminating. Even if the peer review correspondence is included in the publication, it would be helpful to include an explicit remark in the manuscript about the nsp4 instability, as the low nsp4 levels and double bands are quite apparent.

We have explicitly indicated the nsp4 instability issue in our revised manuscript: "Notably, nsp4 appears to be unstable in the absence of nsp3 interaction, as indicated by the presence of double bands and reduced protein levels."

• Regarding the in situ data with the nsp3-4 mutants:
(1) the results seem to indicate that, in some cases, DMVs are formed, although much less abundantly. However, I would be cautious, as cryo-lamellae obtained by FIB-milling represent a miniscule fraction of the cell and are therefore not well suited for quantifications --unless large numbers of lamellae are produced, which is practically unattainable. Consequently, statements like "2/6 cells for the wild-type transfected cells revealed clustered DMVs" (rebuttal) are problematic. Please, consider this when presenting your conclusions in the manuscript.

We agree that cryo-lammellae statistics in this study is limited for quantifications. Our cellular tomography data demonstrate the formation of DMV in the double mutant (V1458E/L1480E). However, it does not exclude the possibility that the quadruple mutant (D1478E/Y1483E/L1486E/Q1490E) can still form DMV, due to limited sample size in this study. We have included a statement in the manuscript to indicate this limitation: "These data suggest charge reversal at the nsp3-4 ectodomain interface affect the capacity of DMV formation, although a larger cellular tomography dataset is required to statistically quantify the effect."

(2) An important point is whether pore complexes were observed in these DMVs, and this should be clearly indicated.

We have included a statement about our observation from the cellular tomography experiment: "The double mutant (V1458E/L1480E) still revealed clustered DMVs and characteristic feature of pore complex (connection between two membranes in DMV) similar to the wild-type,

whereas the quadruple mutant (D1478E/Y1483E/L1486E/Q1490E) exhibited only multi-membrane vesicles and scarce DMV-like vesicles (Extended Data Fig. 8a-b).”

(3) I would strongly recommend avoiding the use of the term “convoluted membranes” here (l. 201). In the coronavirus field, this term typically refers to a distinct type of double-membrane structure induced by coronaviruses, as described in studies such as Knoops et al. (PMID: 18451981). The structures presented in the figures are entirely different and may simply represent residual bodies of the lysosomal pathway.

We thank the reviewer’s correction on this issue and we have rephrased “convoluted membranes” to “multi-membrane vesicles ”.

Other points:

l. 44 “membrane neck” should be “spherule neck”

changed to “spherule neck”

l. 67-68. Please revise the phrasing. Reference 7 did not propose that the complex contained only six copies of nsp3. Indeed, the study detected only the six copies of nsp3 on the crown of the complex, which is perhaps unsurprising given the present structure and the presumed flexibility of the NTDs in the second set of nsp3. However, these six copies nsp3 were proposed to form part of a larger complex that should contain additional components, unidentified at the time.

We have revised the phrase to: “Our structure reveals an unexpected stoichiometry of coronavirus DMV pore complex constituted by twelve copies each of nsp3 and nsp4, whereas the complex was identified to display a 6-fold symmetry and six copies of nsp3 were proposed to form the crown.”

l. 166 six transmembrane helices, not five.

Changed to six.

l. 232-233 mentions conservation of these residues across α & β coronaviruses referring to source data in which only conservation plots of β coronaviruses are included.

We have changed to include only β coronaviruses.

l. 248. Unfinished sentence: “failed to rescue…” what?

Change to “failed to rescue the virus’s capacity of effective replication”.

l. 253. Using “cytoplasmic part of the pore complex” and “luminal part of the pore complex” would be more appropriate than “cytoplasmic pore” or “luminal pore”. Additionally, replacing “pore” with “pore complex”, here and throughout the text may be a better alternative, as “pore” could also refer to just the hollow channel inside the complex.

We thank reviewer’s comment and have updated the phrases throughout the text.

l. 262. While I acknowledge the similarities, I believe it is important to highlight the striking differences. Specifically, the RdRp and capping functions are integrated into the pore complexes of the spherules induced by noda- and alphaviruses.

We agree there is obvious difference on the relationship between RNA replication machinery and RNA translocation activity among these viruses. We include the following discussion in the manuscript: “However, the viral genome synthesis and capping activities are integrated into the pore complexes of the spherules induced by alphavirus and nodavirus. In contrast, coronavirus RNA replication machinery is not an integral component of DMV pore complex, although they might be transiently associated with each other, which warrants further investigation.”

l. 280-281. Please rephrase for clarity. I think the authors are referring to the presence of a CTD domain, which is a feature shared by coronaviruses and arteriviruses. However, the arteri- and coronavirus CTD domains are quite different with no sequence conservations. Additionally, the authors should probably exercise caution in extending their conclusion to the entire Nidovirales order, as the group is rapidly expanding, uncovering unexpected variability in genomes and genome organization (see PMID: 38648214).

We thank the reviewer’s comments and have restricted our conclusion within Coronaviriridae family in Nidovirale. “Considering the conservation of nsp3-CTD and nsp4 among coronaviruses and torovirus in the Coronaviridae family, our structures establish a framework for understanding DMV pore formation and RNA translocation in Coronaviridae family (Fig. 4f), which may even extend to viruses in Arteviridae family of Nidovirale.”

l. 432 non-viable instead of inviable.

Changed.

l. 645 notes 9510% humidity, I assume this is a typo.

Changed.

Referee #3 (Remarks to the Author):

The authors have satisfactorily addressed my concerns.

We thank the reviewer’s comments.